Bull. Min. Res. Exp. (2015) 151: 149-168

Bulletin of the
Mineral Research and Exploration

http://bulletin.mta.gov.tr

DIFFERENTIATION PROCESSES in LATE CRETACEOUS ULTRAPOTASSIC VOLCANICS AROUND AMASYA

Fatma GÜLMEZ[a]* and Ş. Can GENÇ[a]

[a] *Istanbul Technical University Geological Engineering Department, 34469 Maslak, İstanbul*

Keywords:
Late Cretaceous,
Pontides, Ultrapotassic
Magmatism, AFC.

ABSTRACT

Late Cretaceous lithologies around Amasya region are represented by Pontide fore-arc basin units which corresponds a volcanoclastic sequence. This sequence has the products of alkaline ultrapotassic magmatism accompanying calcalkaline lavas which are abundant along Pontide arc. The ultrapotassic rocks which are classified as leucitite, minette and trachyte based on their mineralogical composition, occur as dikes, stocks and rarely lava flows as to be comprised by the Late Cretaceous Volcanoclastic Succession (LCVS). Fractional crytallization accompanied by assimilation (AFC) is a low pressure processes able to differentiate ultrapotassic parental melts to various compositions in a continental margin tectonic setting.The trachytes are the youngest and the most evolved members of LCVS. Therefore we performed AFC modelling using the most primitive minette sample as starting composition and calculated the fractionation trends based on the theoretical mineralogical compositions. We also used the Triassic metapelitic basement rocks of Central Pontides as assimilant. The AFC modelling results imply that it is possible to produce trachytes by adding Central Pontide basement rocks up to 5 %, begining from the most primitive phonolitic sample of Amasya. However the differentiation of leucitite and minette is able to be explained by neither fractional nor assimilation processes.

1. Introduction

An arc environment is defined, which has developed due to the northward subduction of the Neo-Tethys Ocean, during Late Cretaceous in the geological evolution Anatolia located in the Alp-Himalaya orogenic belt (Şengör and Yılmaz, 1981; Okay and Şahintürk, 1997; Yılmaz et al., 1997; Okay and Tüysüz, 1999; Topuz et al., 2013). East-west trending island arc units, namely Pontide arc within the Pontide mountain range form the central segment of this belt that extend along Apuseni-Timok line in Balkans at the west and Sevan-Akera suture belt along the Armenian-Georgian boundary at the east (Adamia et al., 1981; Yılmaz et al., 1997; Georgiev et al., 2009; Mederer et al., 2013). The Pontide arc formation ceased by the collision of Sakarya continent and the Anatolide-Tauride platform or by the Kırşehir Blocks in early Paleocene caused by development of the İzmir-Ankara-Erzincan Suture Belt (IAESZ) (Şengör and Yılmaz, 1981; Okay and Tüysüz, 1999). Pontide arc is represented by calc-alkaline andesitic volcanics, associated pyroclastics and epiclastic units with the I-type granitic intrusions. However, in the southern parts the units of IAESZ and alkali-potassic rocks associated with forearc units are observed. The well-known locations of these alkaline potassic rocks are Ankara-Kalecik, Bayburt-Maden and Amasya-Gümüşhacıköy and the Sinop (Blumenthal, 1950; Alp, 1972). Additionally, recently discovered two outcrops in the west parts of this belt are at around Tosya and Osmancık (Genç et al., 2013). The Amasya region has critical importance due to the three different type ultrapotassic rock suites together with coeval calc alkaline andesites are

* *Corresponding author: Fatma Gülmez, gulmezf@itu.edu.tr*

present. These are identified petrographically as leucitite, minette and trachyte, and are observed in the form of dyke, stock and as lava flows within Late Cretaceous Volcanoclastic Succession together with calc alkaline andesites. This association is not typically observed in aforementioned other regions, except for the Amasya case. For example in Kalecik region, where leucititic and lamprophyric ultrapotassic rocks exhibit an interfingered appearance, but there is no outcrop showing its stratigraphical relationship between trachytic rocks and other potassic rocks. Leucititic rocks are observed in the form of stocks around Gümüşhacıköy. However, lamprophyric and trachytic rocks do not exist in this region. Considering the stratigraphical relationships and outcrop distribution, the Amasya region is the best area unique the potassic/ultrapotassic rock coexistence along the whole belt.

Ultrapotassic rocks are generated in continental rifts or under the control of the extensional tectonism following the continental collision. Its occurrence in active arc environments are limited (McKenzie, 1989; Foley, 1992; Mitchell and Bergman, 1991; Rock, 1991). The best known examples of the potassic volcanic products that accompany the calc alkaline andesitic magmatism are observed in Sunda-Banda, Kamchatka, Japanese and Mexican arcs (Yagi et al., 1975; Luhr and Kyser, 1989; Nelson, 1992). Whereas the increase of the interest and the number of studies focusing on the ultrapotassic magmatism in active subduction zones, there is still debate on which processes forms the ultrapotassic magmatism in the arc environments.

The main aim of this study is to give an example for the rare ultrapotassic magmatism which are the partial melting products of the special mantle sources, in the arc environments from the Central Pontides. The ultrapotassic rocks of the Amasya region were mapped and defined its meaning for the regional stratigraphy. Radiometric age datings, geochemical, isotope and mineral chemistry analysis have been carried out on these rocks. The data obtained from these studies were correlated with the available stratigraphic and paleontological data. Additionally, Late Cretaceous ultrapotassic rocks were classified as leucitite, minette and trachyte by their mineralogical, petrographical and geochemical characters. The petrological models were produced for its differentiation processes from leucitite/minette to trachytic rocks. In order to enlighten of their petrological evolution and crystallization processes.

2. Geology

The very comprehensive study of Alp (1972) and the detailed geological map of Rojay (1995) were used for the stratigraphical relationships of Amasya region ultrapotassic rocks with Late Cretaceous volcanic/volcanoclastic units (Figures 1-2). The Late Cretaceous unit including the ultrapotassic rocks defined collectively as the Kışlacık Group, Karatepe, Geyiközü and Fındıklı formation by previous studies. It was called as the Lokman formation by Alp (1972). The Lokman formation is known as the Everekhanları formation around Bayburt area at the east (Bektaş and Gedik, 1988; Alther et al., 2008). Besides, Kalecik and Gümüşhacıköy vicinities in west form well-known areas in which Late Cretaceous units include leucititic rocks (Bailey and McCallien, 1950; Blumenthal 1950; Çapan, 1984; Tankut et al., 1998; Tüysüz, 1995; Varol, 2013; Eyüpoğlu, 2010). In addition to this ultrapotassic belt located roughly parallel to İzmir-Ankara-Erzincan Suture; it is also necessary to note that the Hamsaros volcanics which contain Cretaceous ultrapotassic leucititic rocks around Sinop (Gedik et al., 1983; Baş, 1986; Asan et al., 2014). The volcanoclastic succession representing the Pontide forearc basin units, is called collectively as "Amasya Late Cretaceous Volcanoclastic Succession (ALCVS).

The basement of ALCVS is formed from the metamorphic rocks of the Tokat Group and overlying Liassic to Lower Cretaceous carbonates known as Vermiş, Ferhatkaya, Sarılar, Carcurum, Soğukçam and Vezirhan formations, and Bilecik Limestone (Alp, 1972; Rojay, 1995; Tüysüz, 1996). The ophiolitic material within Lower Cretaceous carbonates increase towards the Upper Cretaceous units, and turns into an "ophiolitic mélange" (Figure 2). The primary contact relationship of the mélange, which is known as Amasya formation, and ALCVS is documented as an angular unconformity (Alp, 1972; Rojay, 1995; Tüysüz, 1996).

Tüysüz (1996) reported that, the pelagic carbonate depositions began following the rift volcanism continued until Late Jurassic in the region. He also states that this sedimentation is similar to a passive continental margin deposition, and could be correlated with western part of Sakarya Continent. Rojay (1995) subdivided the carbonates (the Amasya Group) as; the Early Jurassic bioclastic carbonates, the Middle Jurassic regressive carbonates containining the Ammonitico Rosso at the bottom and the Early Cretaceous pelagic carbonates. He also argues that the

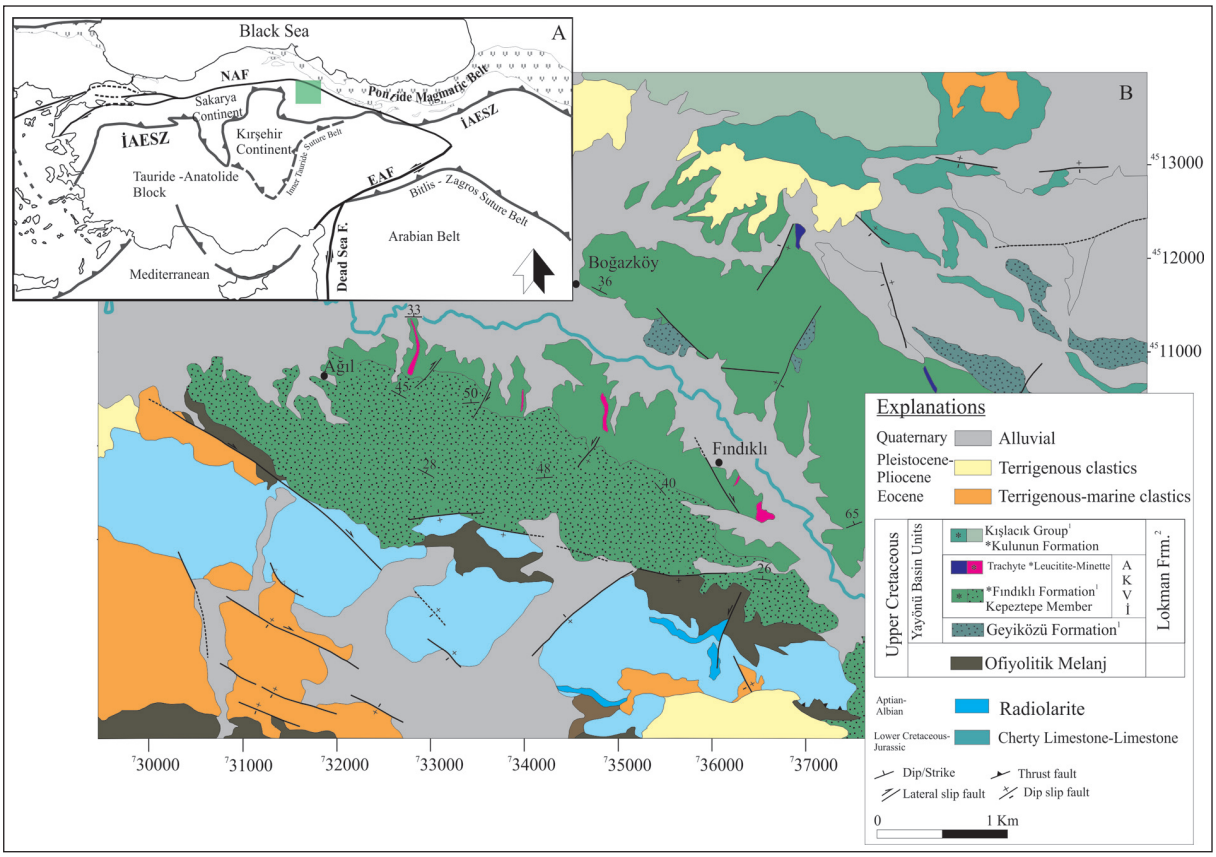

Figure 1- a) Location of the study area within general tectonic units of Anatolia (EAF: East Anatolian Fault Zone, IAESZ: Izmir-Ankara-Erzincan Suture Zone, DSF: Dead Sea Fault; Okay and Tüysüz, 1999; Ciobanu et al., 2002; Şengör et al., 2005; Sosson et al., 2010; Mederer et al., 2013) and b) Outcrops of ALCVS ultrapotassic rocks in the geological map prepared by Rojay (1995) (1: Rojay, 1995; 2: Alp, 1972).

platform, which gradually uplifted starting from Liassic, began to collapse in a deepening environment by the sudden rise of the sea level in Middle Jurassic. Rojay also emphasizes that this depositional environment was a passive continental margin, then turned into a converging plate margin in Campanian-Maastrichtian by the mélange obduction. Yılmaz et al. (1997) pointed out the limestone deposition followed by the red pelagic limestone, mudstone and radiolarite deposition during Cenomanian-Turonian period. According to these authors, this passed gradually into a wild flysch at the top by the incorporation of older limestone blocks and olistostromes, together with the blocks and slices from the ophiolitic mélange (Yılmaz et al., 1997).

ALCVS' outcrops are seen between Lapköyü at the north and Fındıklı village at south (Figure 1). It is observed that the unit begins with flysch-like sediments at the bottom, and grades into an epiclastic unit containing mostly andesitic lava pebbles. These materials are badly sorted and cemented by a mudstone, siltstone and sandstone matrix. In this paper, "volcanoclastic sediment" or "epiclastic" definition describe the non-volcanic products formed from the deposition by erosion and transportation processes (Reading, 2009). ALCVS epiclastic unit, covers all the different rock name, such as andesitic breccia, agglomerate, tuff/tuffite, pyroclastic and volcanic breccia in previous studies (Alp, 1972; Koçyiğit, 1988; Tüysüz, 1996). The "true" volcanic/pyroclastic units are beyond of this description. Field studies revealed that flysch type sediments and epiclastic units show lateral and vertical transitions. Epiclastic rocks were formed when large amounts of volcanic material is transported into the basin. Decreasing of the volcanic materials, normal flysch deposition occurred. Although the epiclastic unit is monogenetic, it also contains some leucitite and minette pebbles. In the northern areas, abundant trachyte pebbles are found to the top of the succession. Andesitic lava flows are also widespread within the volcanoclastic succession (Figure 2).

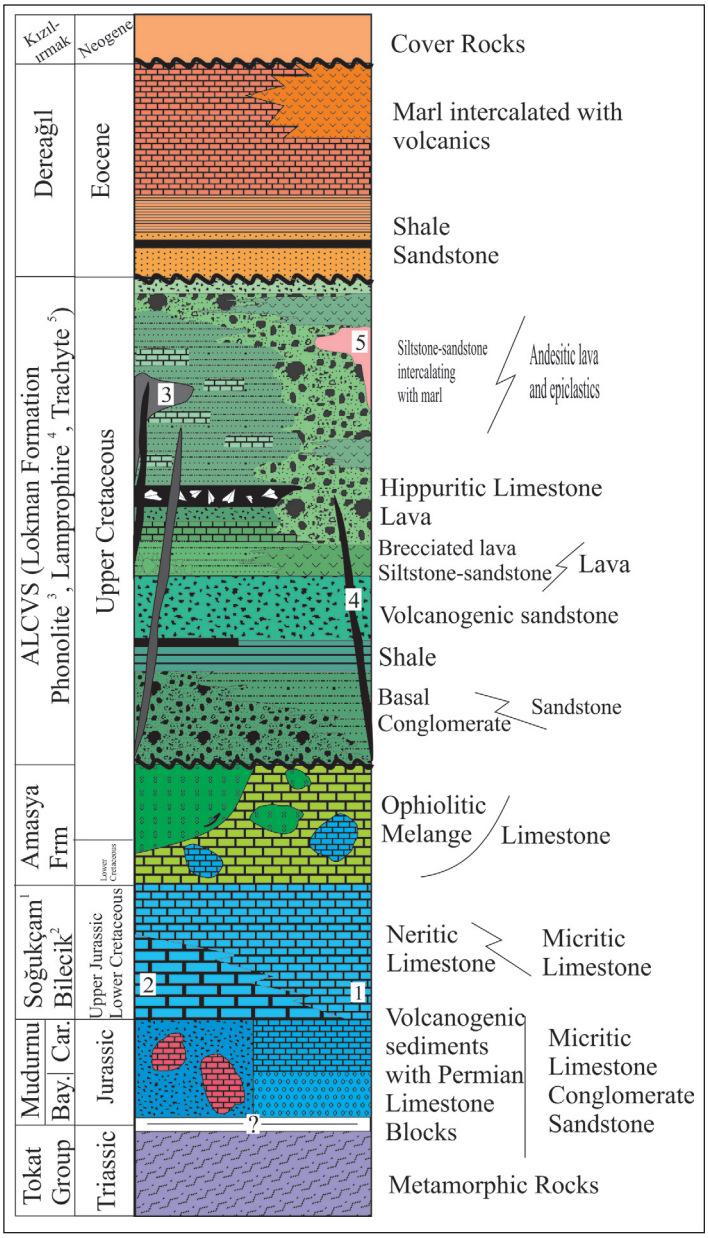

Figure 2- Stratigraphic relationship between leucitite, lamprophyre and trachytes within non-scaled, generalized stratigraphic section of Amasya and surroundings (after Alp, 1972).

There are abundant and reliable fossil findings from the ALCVS to determine its age. Alp (1972) reported the age of unit, based on macro fossils (*Actaeonella* sp., *Hippurite* sp.) rather than micro fossils as Campanian-Maastrichtian. However; Koçyiğit et al. (1988) dated units as Lower Companian-Maastrichtian in age. Asan et al (2014) carried out $^{40}Ar/^{39}Ar$ age datings from the phlogopitic micas of two shoshonitic rocks as 82.08 ± 1.13 and 81.37 ± 0.81 My. These ages are in a good agreement of the paleontological data.

3. ALCVS Magmatic Rocks

3.1. Leucitite

The outcrops of the leucitites are observed as small stocks and dikes, along Yeşilırmak valley in the south of Boğazköy (Figure 3a). These are generally yellowish to white gray colored and highly altered. These are massive and pale gray colored in relatively more fresh outcrops. Leucite crystals are dull, and pale pink-whitish in color, and embedded into the

groundmass (Figure 3b). Euhedral, bright and pink colored leucite phenocrysts, 1-2 cm in diamaters are typical. Joint sets, beddings, columnar joints or other structural features are not observed in stocks. Columnar joints developed in 1.5 m wide leucitite dike (Figure 3a). Leucitite pebbles and/or blocks are also observed within the epiclastic rocks of the ALCVS.

3.2. Minette

Minette type lamprophyres crop out in the form of NW-SE or NE-SW trending dikes, located in the south of Yeşilırmak valley and cut the epiclastics, and there are no continuations to the northern side of the valley. The northernmost of the study area, an aphyric minette dike cutting the trachyte dome is present. The width of minette dykes varies between 40 cm to 2 m. Pinkish to pale brown colors due to the feldspars and shining views because of micas are typical in hand specimens (Figure 3d). Minettes cut the epiclastic rocks and interfingered with the leucititic stock (Figure 3c). Presence of a sharp contact with leucitites has not been identified. Possibly these two rocks are transitional with each other, observed in the leucitic lamprophyre and phlogopite lamprophyre dikes of the Ankara-Kalecik area (Gülmez et al., 2014*a*).

3.3. Trachyte

Trachytes, which are the youngest ultrapotassic products of ALCVS, are observed in the form of 5 m wide, NW-SE oriented dyke around Kelışığın Hill in

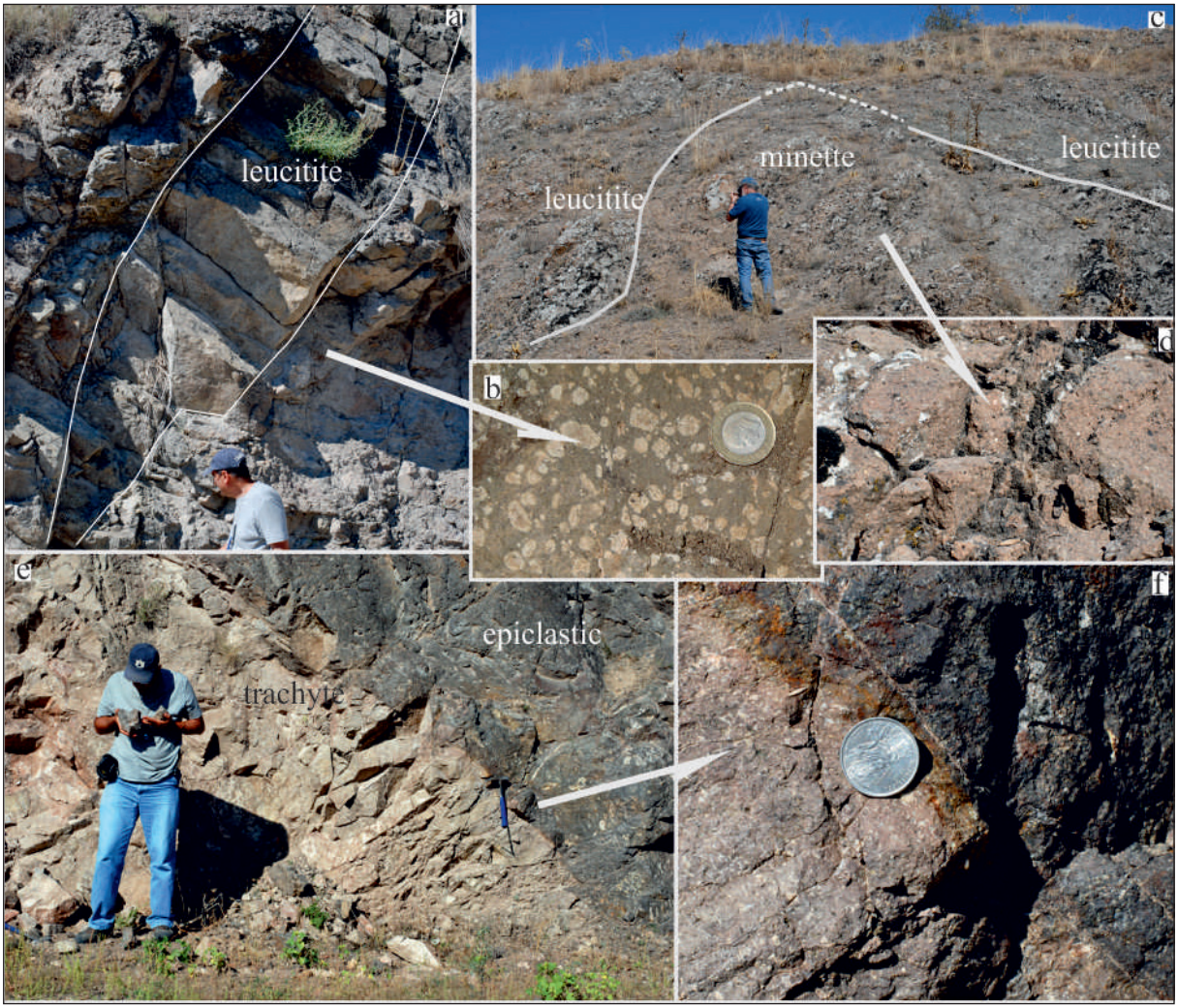

Figure 3- Outcrop views of ultrapotassic rocks a) columnar jointing forms in leucitite lava, b) leucitites in hand samples, c) general outcrop view from minette stock, d) minette in hand samples, e) the contact between trachytic dome and epiclastic units, f) the chill zone developed along the contact.

north of Yeşilırmak valley, and as a small dome around Lapköyü. Trachytic rocks are recognized with their pink color, and massive appearances (Figures 3 e-f). Coarse (upto 2 cm), euhedral prismatic feldspar phenocrystals and trachytic textures which can be observed even in hand specimens are typical for trachytes. It was observed that glassy, dark colored, partly aphyric or micro crystalline margin zone (quenching zone) at the contact of trachytic dome with epiclastic unit (Figure 3f). This zone is continuous along the contact and its width does not exceed 2-5 cm. The hypabyssal and plutonic equivalents of the unit have been documented by Alp (1972) in the NE of Amasya.

3.4. Andesites

Andesites are observed in the form of lensoidal lava flows having thicknesses not exceeding 1 m, which do not exhibit lateral continuity within epiclastic units. It alternates with the epiclastic units, and rarely cut them. They have generally massive and are gray colored on their fresh surfaces. On the alteration surfaces their colors can be reddish, brownish or greenish gray. They are also represented by the flow breccias at the bottom of the lava flows road between Boğazköy and Lapköyü. They are along the road highly altered and characterized by porphyric textures in hand samples with the relatively coarse plagioclase phenocrystals.

4. Radiochronological Findings

Radiochronological studies have been made on 1 trachytic, 1 leucitic and 2 minette type rocks in order to provide stratigraphical correlation. Sanidine and whole rock in trachytic sample, phylogopite in minettes, and leucites in leucitite were analyzed. The alteration of the mineral, the presence of another mineral or fluid inclusions, whether it exhibits compositional zoning and changes due to reactions on edges were taken as basis in the selection of minerals which are suitable for analyze. Samples were subjected to the radiation as described in the study of Dalrymple et al. (1981) in McMaster nuclear reactor in Ontario Hamilton for the production of ^{39}Ar from ^{39}K. The radiometric $^{40}Ar/^{39}Ar$ dating analyses were performed following the methods in the study of Hames et al. (2009) in the laboratories of the Auburn University (ANIMAL: Auburn Nobel Isotope Mass Analysis Laboratory). Results were evaluated by Microsoft Excel and Isoplot software (Ludwig, 2003).

Results of the analysis have been compatible with the results of previously performed stratigraphical and paleontological studies in the region. According to the results obtained from phylogopite analyses, the plateau ages determined for the minettes range between 76.78 ± 0.19 and 77.43 ± 0.15 My (Figures 4 a-b). The plateau age obtained from K-feldspars in trachyte sample is 75.83 ± 0.09 My (Figure 4c). In addition, the whole rock age determination carried out in the same sample is 70.1± 1.3 My. The plateau age could not be detected as the K amount of leucites is low because of analcimization in leucitites. Total gas age data obtained from the crystals that have spherulitic and radial K-feldspar rims, is 75.6 ± 3.7 (Figure 4d). Although there is a high error in the radiometric data obtained due to low K amount, this finding is also compatible with other findings and probably point out the crystallization age of hypocrystalline K-feldspars in groundmass.

5. Petrographical Characteristics and Classification

In the classification of volcanic units in ALCVS, studies of Le Maitre (2002) and Mitchell and Bergman (1991) were taken as basis. Accordingly; four different Late Cretaceous lithological units were defined in Amasya.

5.1. Leucitite

The general mineralogical composition of leucitites were determined as clinopyroxene+ leucite±alkali feldspar+apatite+magnetite by petrographical investigations. As secondary minerals; analcime, calcite, sericite, clay and opaque minerals were observed. Leucites are generally observed as coarse (1-3 cm in size) and in the form of idiomorphic phenocrysts. There are zones, made up of alkali feldspar, which developed as a result of the reaction with groundmass around the edges of euhedral leucites in glassy groundmass and grew radially (Figures 5 a-b). They typically exhibit isotropic behavior in crossed nicols. Leucites form the groundmass in some samples and have completely transformed into analcime (Figures 5 c-d). In studies of mineral geochemistry, the findings of fresh leucite phenocrystal or microcrystal were not encountered (Gülmez et al., 2014*b*). The mafic phase of leucitites in diopsitic composition is clinopyroxene (Figures 5 c-d). They are observed in the form of idiomorphic-hipidiomorphic, dark or pale green colored, and fissured micro/phenocrysts. Simple, penetrative or hourglass twinning, compositional zoning and

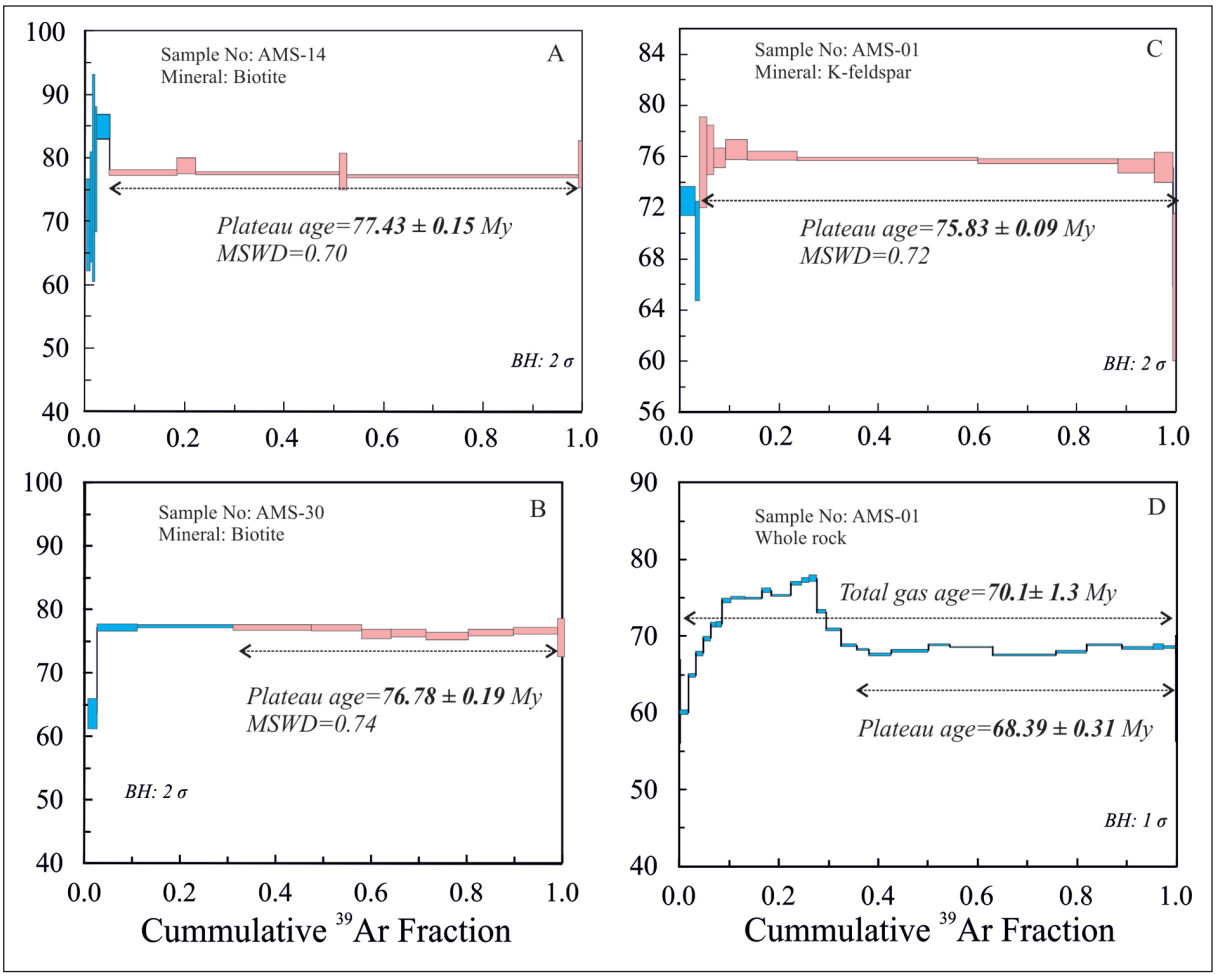

Figure 4- The age spectrum for ALCVS lavas in this study (See text and spectra for explanations, BH: Box Height, MSWD: Mean Square Weighted Distribution value).

corrosive textures, of which leucites have caused in some crystals, are widespread. They have glass and opaque minerals inclusions. Feldspar bearing leucitites are rare, and these samples do not contain feldspar as phenocrysts. Feldspar is generally observed as a cryptocrystalline matrix phase in leucitites, and causes development of spherulitic reaction textures along the rims of analcimes (Figures 5 a-b). Apatites, which are the most widespread accessory mineral of leucities are typical with their prismatic forms, and are located in groundmass as crystals or mainly as enclaves within phenocrysts.

Leucitites are generally observed both as hipocrystalline porphyric texture, characterized by the coarse leucite phenocrysts embedded in the glassy matrix. The development of devitrification texture in glassy groundmass and spherulitic texture along the rims of leucites are widespread (Figures 5 a-b). The formation of cumulate texture is also observed as a result of clustering of leucite microcrystals.

5.2. Minette

Although minette type rocks are intermingled with leucitites in outcrop scale, they differ from leucitites by lack of the leucite from the point of mineralogical composition. Their main mineralogical compositions are as follows; clinopyroxene+mica±K-feldspar+opaque mineral. As secondary minerals; calcite, clay minerals, sericite and zeolites are seen.

Mafic minerals of minettes are clinopyroxene and mica (Figures 5 e-f). Pyroxenes are the prevailing mafic mineral phase of minettes like in leucitic rocks. Although it is considered that some six-sided pseudomorphs could be olivine, the finding of fresh olivine has not been encountered. The formation of alteration related secondary calcite, zeolite and clay

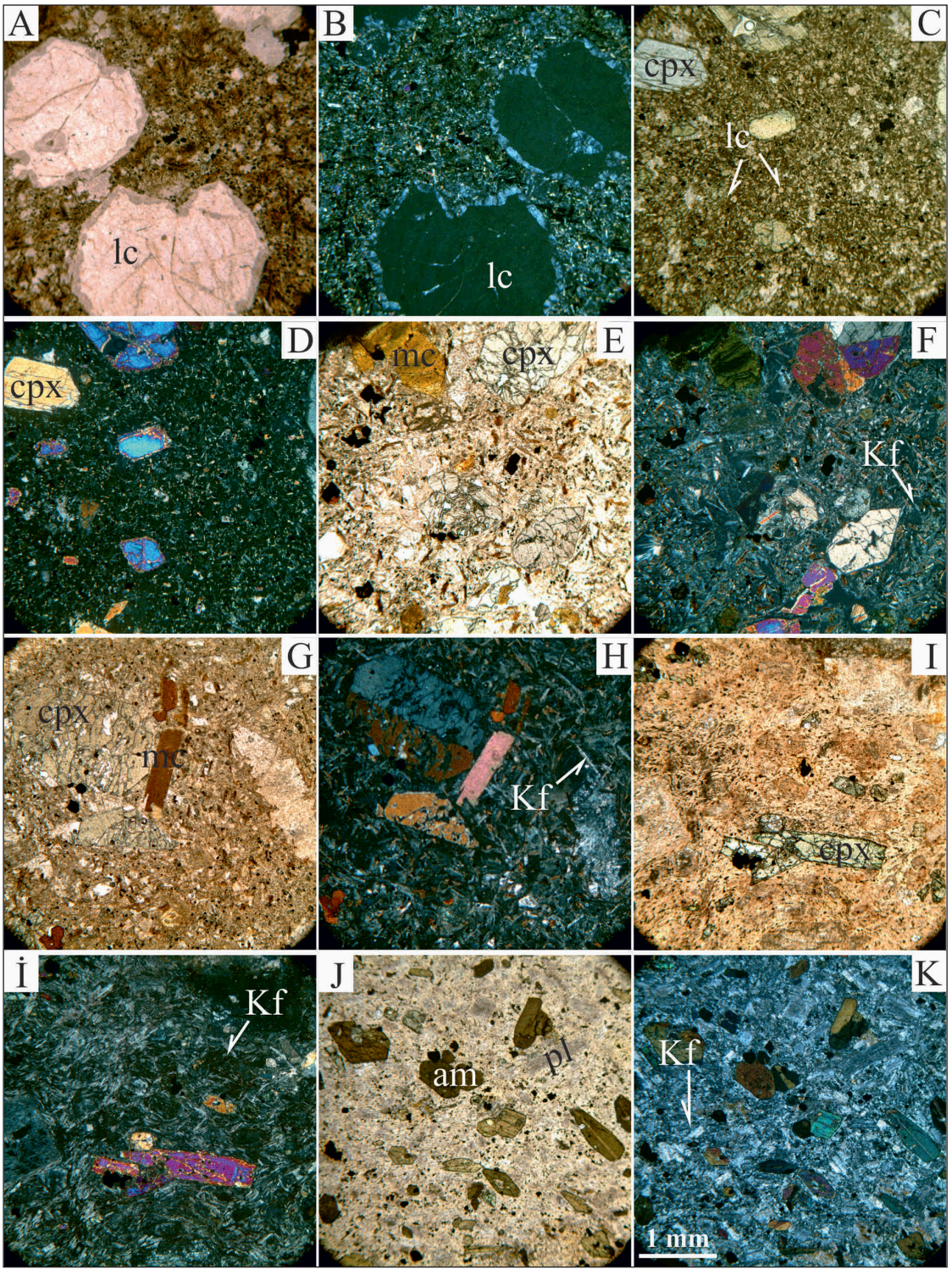

Figure 5- The thin section views of ALCVS lavas (all photos were taken by 4x magnification and the scale given in K is valid for all photos), a-b) leucite crystals under plane and cross polarized light, c-d) leucite microphenocrystals as groundmass phases, e-f) clinopyroxenes in minettes under plane and cross polarized light plane and cross polarized light, g) prismatic mica phenocrytals in minette, h) simple twinning clinopyroxene phenocrystal and Kf microliths as groundmass phases in minette sample, ı-i) trachytic texture in trachytes which contain clinopyroxene accompanies mica as mafic phase, under plane and cross polarized light, j-k) euhedral amphiboles in amphibole-bearing trachytes, altered plagioclase under plane polarized light and Kf microcrystals under cross polarized (lc: leucite, cpx: clinopyroxene, Kf: K-feldspar, pl: plagioclase, am: amphibole).

minerals are abundant in samples. Feldspars are in the form of prismatic rods, and they cause the rock to appear in pink color in hand samples (Figure 5g). They are typical with their alteration related, yellowish, simple twins and low, double refraction colors. Clinopyroxenes are similar to those of the leucitite samples, and they are represented by coarse phenocrystals or as microcrystals in groundmass. Unequilibrium textures around the rims of coarse pyroxene crystals and glass inclusions oriented closer to the outer parts of the crystals, are abundant. Zoning, simple and lamellae twinning are the other typical characteristic of pyroxenes (Figure 5f). Micas are generally phlogopite in composition (Gülmez et al., 2014*b*), and provide minettes to be easily defined in hand samples. In hand samples, they are observed as golden yellow in color. It is characterized by their perfect cleavage in one direction, strong pleochroism and parallel extinction (Figure 5g). Magmatic corrosion or alteration is not observed in phenocrysts. However, the slightly alteration and opacitized rim development is abundant in micas (in samples which are observed as pebbles in epiclastic units). Flow controlled bending and buckling of the micas are also identified in thin sections. Minettes exhibit the holocrystalline, porphyric, intergranular textures. The development of fluidal texture originating from feldspar laths can be seen in the groundmass. As some samples contain very fine grained micro/phenocrysts, they have been defined as aphyric texture.

5.3. Trachyte

Trachytic rocks in the study area can be characterized by the composition of feldspar+ plagioclase±amphibole±mica±clinopyroxene+apatite +sphene+opaque minerals. They are divided into two groups according to their mafic mineral compositions as; a) amphibole (and minor pyroxene) trachytes, and b) mica-pyroxene trachytes. As secondary minerals; calcite, sericite, chlorite and clay minerals are abundant. Sanidine is the dominant feldspar type of trachytes (Figure 5ı-k). Sanidines are observed as microliths or as prismatic phenocrysts reaching 1 cm, and they sporadically form trachytic texture (Figure 5ı-i). Amphibole inclusions are observed in sanidines. Amphiboles, which are observed as euhedral in many samples, were defined as hornblende petrographically (Figure 5j). Pyroxenes are present in the form of altered phenocrysts reaching mostly 1 mm in size or microphenocrysts within groundmass (Figure 5ı-i). Fissured and altered pyroxenes are in diopsitic composition as it was in other ultrapotassic rocks. Micas of the trachytic rocks show similarities with phlogopites in minettes in terms of yellowish, bronze colors. However; it needs for mineral chemistry study for true classification. As accessory phase, apatite crystals, which reach 1 mm size, and wedge shaped, prismatic or anhedral sphene minerals were identified.

Trachytes display idomorphic-hipidiomorphic, hipocrystalline, porphyric in texture, and trachytic (fluidal) texture development is apparent in some samples. Poikilitic texture, by which amphibole inclusions, is characteristic in feldspars.

5.4. Andesite

Andesitic rocks are generally presented by clinopyroxene+plagioclase+mica±K-feldspar+ opaque mineral assemblage. Calcite, zeolite and clay minerals as secondary minerals accompany to those primary minerals. The main feldspar type is the plagioclase. In order to determine its types optical measurements were carried out. According to extinction angle, it was determined that plagioclases are An_{45-60} in composition. Zoning and polysynthetic albite twinning is typical for the plagioclases. They are observed as altered, prismatic microphenocrystals or as microliths in the groundmass. Mica microphenocrysts, which are observed as almost fully opacitized, are in prismatic forms. Andesitic lavas are hipocrystalline, porphyric and microlithic in texture. Rarely subophitic texture which characterized by the clinopyroxene and plagioclase interfingering is also noted.

6. Whole Rock Geochemistry

Major and trace element analysis of whole rock samples of ALCVS volcanic rocks are shown in the table 1. Due to its submarine setting, the volcanic rocks have been severely affected by various alteration processes. Additionally some weathering processes which are obvious on petrographic thin sections of samples, are not unexpected after considering the age of rocks. We selected the most freshest representative 16 samples and prepared them for whole rock geochemical analysis, and then sent to ACME laboratories in Canada. Major oxides and trace elements including rare earth elements were analyzed by ICP-AES and ICP-MS, respectively. For analyses, the mixture of 200 g. powdered sample and 1.5 g. $LiBO_2$ were melted in an oven under 1050°C temperature, and the melt was then taken into 100 ml,

5% HNO_3. The solution prepared for each sample and the international standards for the calibration were also analyzed (W-2, AGV-1, GSP-2, BCR-2 and STM-1).

The SiO_2 vs. K_2O+Na_2O diagram (TAS: Total Alkali versus Silica), which the most common classification diagram for magmatic and volcanic samples with water-free oxide contents normalized to 100% are plotted on (Le Matire, 2002). We also classified ALCVS volcanic rocks on TAS diagram of Le Bas et al. (1986) (Figure 6a). However, we avoided to calculate water-free contents not to cause SiO_2 contents of the samples to increase dramatically as it would mask the silica undersaturated nature of the ALCVS ultrapotassic rocks, due to their high LOI (Loss of Ignition) values (Rock, 1991). Additionally, the readers should keep in mind TAS classification for ALCVS ultrapotassic rocks is just for an idea at first glance due to the fact that the diagram does not satisfy the requirements of the ultrapotassic and high potassium rock classification in terms of that complex mineral paragenesis and high potassium contents of ultrapotassic rocks (Conticelli et al., 2013). In this diagram, leucitic of ultrapotassic rocks plot on tephrite, tephri-phonolite fields; minettes plot on trachy-basalt, basaltic trachy-andesite, tephri-phonolite fields; andesitic rocks plot on basaltic–andesite and trachy-andesite; trachytic rocks

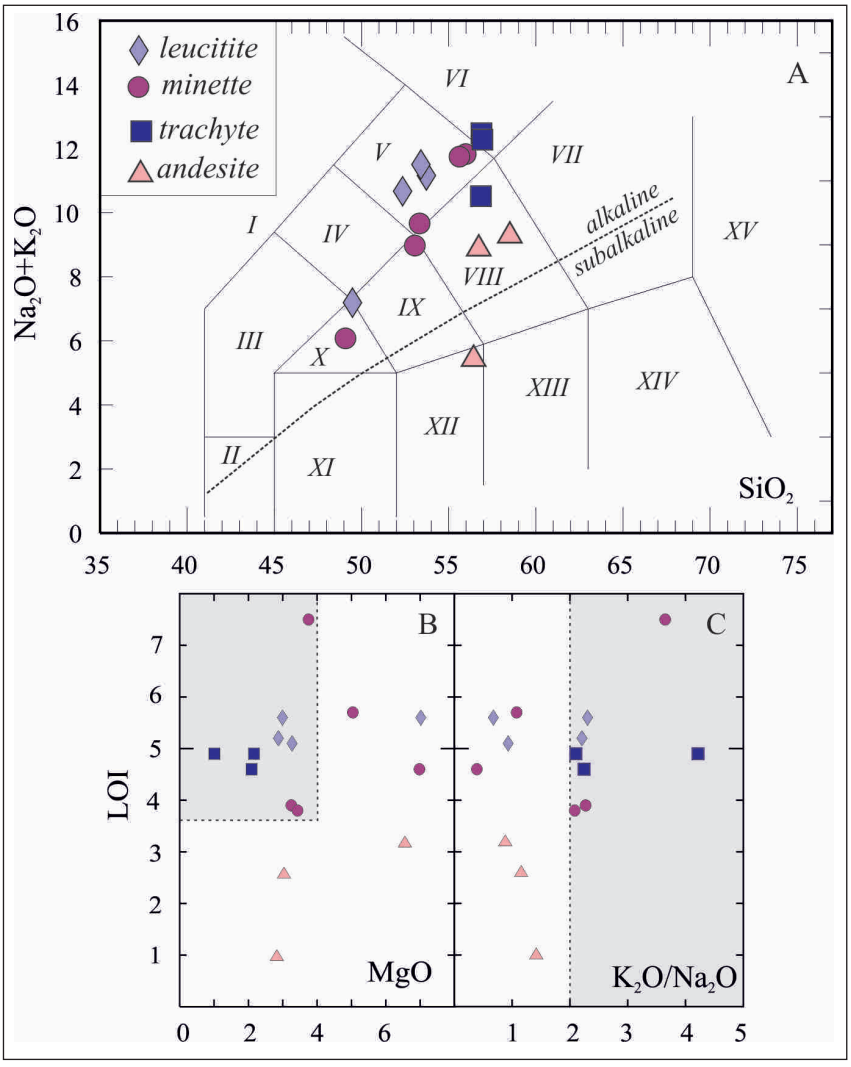

Figure 6- a) The classification of ALCVS ultrapotassic rocks on total alkaline vs. silica diagram (Le Bas, 1986), b) the variation of LOI % with K_2O/Na_2O ratio for leucitites, minettes and trachytes, c) the variation of LOI % with MgO % for leucitites, minettes and trachytes (gray colored area represents samples that yield $K_2O/Na_2O > 2$ condition).

Table 1- Whole rock major, minor and trace element analysis with calculated CIPW norms for Amasya sample.

Sample No	AMS-07	AMS-11	AMS-32	KT-34A	AMS-14	AMS-30	KT-36D	KT-33A	AMS-29	AMS-01	AMS-28	AMS-19	AMS-21	13_05
x	732040	736555	736541	733093	736640	736393	732805	733093	738157	736967	738157	738157	741380	736666
y	4511575	4510507	4510498	4512124	4510200	4510610	4512295	4512124	4511762	4513275	4511762	4511762	4510321	4512961
Rock Type	Leucitite				Minette					Trachyte			Andesite	
SiO_2	49,06	50,35	49,87	46,03	49,49	53,27	52,96	46,13	48,71	53,59	53,81	53,57	53,96	54,66
TiO_2	0,73	0,68	0,69	0,92	0,77	0,64	0,67	1,03	0,92	0,51	0,52	0,51	0,98	0,95
Al_2O_3	17,87	18,34	18,22	13,21	13,82	18,77	18,70	12,99	16,79	18,92	18,7	19,04	12,26	17,37
Fe_2O_3	7,75	6,67	6,53	10,14	7,90	6,03	6,17	10,96	7,9	4,84	4,69	4,62	7,98	6,86
MnO	0,17	0,16	0,15	0,19	0,15	0,13	0,13	0,20	0,27	0,17	0,17	0,14	0,16	0,17
MgO	3,27	2,87	2,99	7,02	5,04	3,25	3,43	6,98	3,75	2,16	2,09	1,01	6,50	2,98
CaO	4,79	4,38	4,37	9,33	8,11	2,04	2,20	10,52	4,45	2,57	3,2	5,72	9,03	5,10
Na_2O	5,18	3,26	3,25	3,99	4,03	3,44	3,63	4,11	1,9	3,79	3,58	1,9	2,76	3,98
K_2O	4,82	7,2	7,49	2,7	4,34	7,82	7,56	1,60	6,93	7,97	8,03	8,01	2,43	4,57
Cr_2O_3	<0.002	<0.002	<0.002	0,011	0,026	0,003	0,003	0,016	<0.002	<0.002	<0.002	<0.002	0,085	0,004
P_2O_5	0,84	0,47	0,46	0,49	0,38	0,37	0,37	0,54	0,5	0,17	0,18	0,16	0,27	0,39
LOI	5,1	5,2	5,6	5,6	5,7	3,9	3,8	4,6	7,5	4,9	4,6	4,9	3,2	2,6
Total	99,59	99,61	99,61	99,62	99,71	99,67	99,67	99,63	99,6	99,58	99,59	99,53	99,63	99,61
CIPW														
Quartz	0,00	0,00	0,00	0,00	0,00	0,00	0,00	0,00	0,00	0,00	0,00	0,18	6,62	1,20
Orthose	28,48	42,55	44,26	15,96	25,65	46,21	44,68	9,46	40,95	47,10	47,45	47,34	14,36	27,01
Albite	25,32	15,99	12,67	18,48	19,69	23,83	23,48	23,25	16,08	20,39	19,58	16,08	23,35	33,68
Anorthite	11,27	14,14	13,00	10,16	6,80	7,70	8,50	12,27	16,82	11,07	11,24	19,77	13,89	16,03
Leucite	0,00	0,00	0,00	0,00	0,00	0,00	0,00	0,00	0,00	0,00	0,00	0,00	0,00	0,00
Nepheline	10,03	6,28	8,03	8,28	7,81	2,86	3,92	6,25	0,00	6,33	5,80	0,00	0,00	0,00
Diopside	3,99	2,16	3,00	23,71	22,46	0,00	0,00	26,15	0,00	0,00	1,80	4,93	20,52	3,17
Wollastonite	0,00	0,00	0,00	0,00	0,00	0,00	0,00	0,00	0,00	0,00	0,00	0,00	0,00	0,00
Hypersthene	0,00	0,00	0,00	0,00	0,00	0,00	0,00	0,00	2,16	0,00	0,00	0,23	6,68	5,95
Olivine	4,41	4,31	4,24	4,55	1,50	5,67	5,99	3,69	5,03	3,77	3,06	0,00	0,00	0,00
Ilmenite	0,36	0,34	0,32	0,41	0,32	0,28	0,28	0,43	0,58	0,36	0,36	0,30	0,34	0,36
Hematite	7,75	6,67	6,53	10,14	7,90	6,03	6,17	10,96	7,90	4,84	4,69	4,62	7,98	6,86
Sphene	0,00	0,00	0,00	0,00	0,00	0,00	0,00	0,00	1,41	0,00	0,00	0,87	1,96	1,86
Perovskite	0,92	0,85	0,89	1,20	1,02	0,00	0,00	1,37	0,00	0,28	0,56	0,00	0,00	0,00
Rutile	0,00	0,00	0,00	0,00	0,00	0,49	0,52	0,00	0,04	0,16	0,00	0,00	0,00	0,00
Apatite	1,99	1,11	1,09	1,16	0,90	0,88	0,88	1,28	1,18	0,40	0,43	0,38	0,64	0,92
Sc	9	8	8	33	21	8	8	36	11	4	5	4	33	17

Table 1- (*continued*)

Co	24,3	17,5	17,3	35,4	23,4	15,5	15,6	37,7	19,5	9,1	9,2	8,9	35,9	18,7
Cs	11,9	4,7	4,1	6,5	5,7	4,2	4,1	4,0	10	18,0	17,7	1,2	0,6	5,0
Ga	16,9	19	17,7	15,6	13,1	16,7	16,1	15,8	20,8	15,5	16,1	18,5	14,5	21,7
Hf	3,1	2,9	3,2	3,2	3,6	4,1	3,9	3,4	4	3,6	4,1	4,2	3,4	5,1
Nb	10,7	15,8	14,4	8,8	9,5	18,2	17,2	8,8	14,1	13,6	13,5	14,1	7,7	16,2
Rb	134,1	279,2	279,5	61,2	89,9	217,7	207,7	99,7	173,9	191,6	199	205,4	54,9	118,8
Sr	845,5	925,2	791,1	533,2	369,9	604,1	578,5	454,9	664,3	825,2	1031,4	1677,9	700,1	889,0
Ta	0,5	0,8	0,9	0,6	0,5	0,9	1,1	0,4	0,7	0,7	0,8	0,7	0,6	0,9
Th	12,5	12,6	11,6	9,2	10,6	15,1	15,2	8,5	9,3	13,7	13,4	13,9	7,7	17,2
U	6,7	4,6	4,5	3,4	3,4	5,0	4,9	3,0	2,8	3,7	4,5	5	2,9	3,2
Zr	127,5	144,3	145	112,2	140,6	172,4	166,5	115,9	168,6	157,7	156,8	158,7	102,2	214,8
Y	21,9	20,6	20,2	24,8	20,7	19,5	20,9	27,1	26,9	21,8	22	22,9	20,7	25,0
La	40,9	39,7	38,2	33,5	37,7	41,5	39,9	33,6	41,2	44,3	42	43,9	27,0	40,9
Ce	81,5	73,8	71,8	66,5	74,1	77,9	77,2	69,8	76,3	77,8	72,9	73,4	54,7	87,9
Pr	9,19	8,58	8,46	8,21	8,12	8,24	8,14	8,90	9,22	7,93	8,03	8,13	6,35	9,60
Nd	37,3	33,4	32,8	32	30,8	29,9	30,9	39,7	35,6	28,8	31,7	31	25,0	38,0
Sm	7,44	7,21	6,53	8,32	6,58	5,87	5,86	8,90	7,77	5,67	5,87	5,95	5,32	8,13
Eu	1,83	1,77	1,85	2,14	1,72	1,57	1,57	2,30	2,16	1,63	1,74	1,71	1,44	2,16
Gd	6,29	5,8	5,64	7,42	5,80	4,83	5,02	7,91	6,62	4,87	5,14	5,11	4,89	7,10
Tb	0,92	0,81	0,8	0,97	0,84	0,75	0,77	1,21	0,99	0,79	0,79	0,77	0,77	0,97
Dy	3,87	4,16	3,95	5,26	4,13	3,79	3,57	5,42	5,21	4,13	4,37	4,15	3,77	4,93
Ho	0,89	0,82	0,76	0,8	0,82	0,78	0,80	1,05	0,97	0,83	0,8	0,78	0,82	0,84
Er	2,03	1,89	2,05	2,15	1,93	2,26	2,11	2,69	2,58	2,36	2,09	2,26	2,22	2,49
Tm	0,32	0,32	0,31	0,36	0,31	0,37	0,35	0,34	0,37	0,40	0,34	0,34	0,34	0,34
Yb	1,83	1,76	1,91	1,79	1,75	2,14	2,02	2,06	2,58	2,29	2,27	2,32	1,87	2,14
Lu	0,31	0,29	0,28	0,3	0,32	0,38	0,33	0,32	0,35	0,35	0,37	0,34	0,33	0,33
Pb	25,8	18,7	21,2	13,1	10,3	21,6	22,2	12,1	4,8	14,7	14,8	24,5	18,5	14,1
Ni	7,0	4,2	3,6	17	27,6	6,9	6,8	17,2	1,4	3,4	3,4	2,9	53,9	9,0

plot on trachy-andesite and phonolite fields. However the samples which plot on the fields of trachy-basalt, basaltic trachy-andesite and trachy-andesite, satisfy the condition of $Na_2O - 2 \leq K_2O$, then they were given the names of trachy-basalt, shoshonite and latite (Le Maitre, 2002).

Except a few andesitic samples, the ALCVS volcanic rocks are in alkaline character. Leucitite and minette type rocks display similar major and trace element variations and no significant diversification on Harker-variation diagrams while trachytic rocks are silica-saturated and always represent the most enriched end members. K_2O/Na_2O values in all three rock groups, are quite variable ($0.4 < K_2O/Na_2O < 4.2$). Although leucitites, minettes and trachytes of ALCVS display the effects of alteration since they are the product of an old submarine volcanism, the lack of the marked correlation between LOI with K_2O (Figure 6 b) demonstrates that high K_2O % values have not developed due to the alteration. Beside that some of the samples with the highest MgO% (>5) and highest LOI values, have relatively low K_2O/Na_2O (< 2) ratios, are the evidences showing the migration of potassium to some extent (Figure 6c). Especially, the analcimitization was very thorough processes for leucitites, have caused loss in potassium and gain in sodium in significant amount. However, since there is no any other Na-bearing mineral phase except the analcime in leucitites, the most of Na_2O % contents of these samples could be interpreted as their primary K_2O % values. Additionally high degree carbonatization in minettes and sericitization in trachytes were very common. Although the variable effects of alteration processes on rock groups and their whole rock geochemistry, primary mineral paragenesis of ALCVS volcanic rocks suggest that leucitites, minettes and trachytes are obviously ultrapotassic in character. This is also evident by the modal mineralogical compositions estimated based on CIPW norms that have revealed that leucitites and minettes are Ne-normative (2.28-10.03%). In classical potassic rock classification diagrams of Foley et al., (1987), ALCVS leucitite, minette and trachytes plot on the area resembles Roman Province potassic rocks (Figures 7 a-b).

Leucitite, minette and trachytes display significant enrichment of Large Ion Lithophile (LIL) elements and depletion of High Field Strength (HFS) elements on N-MORB normalized multi-element diagrams (Figure 8). Negative anomalies of Nb and Ta are common for each rock groups. For comparison, one representative calcalkaline andesitic sample is also plotted on each diagram (Figure 8). The patterns of ALCVS ultrapotassic rocks on N-MORB multi-element diagrams (Figure 8a-c) are typical for subduction related rocks. They are also similar with the Enriched Mantle (EM) and with the Oceanic Island Basalts (OIB) in terms of their Ta/Yb and Th/Yb ratios (Figure 9 a), and compared with arc volcanics in terms of their Th contents with Ba/Th

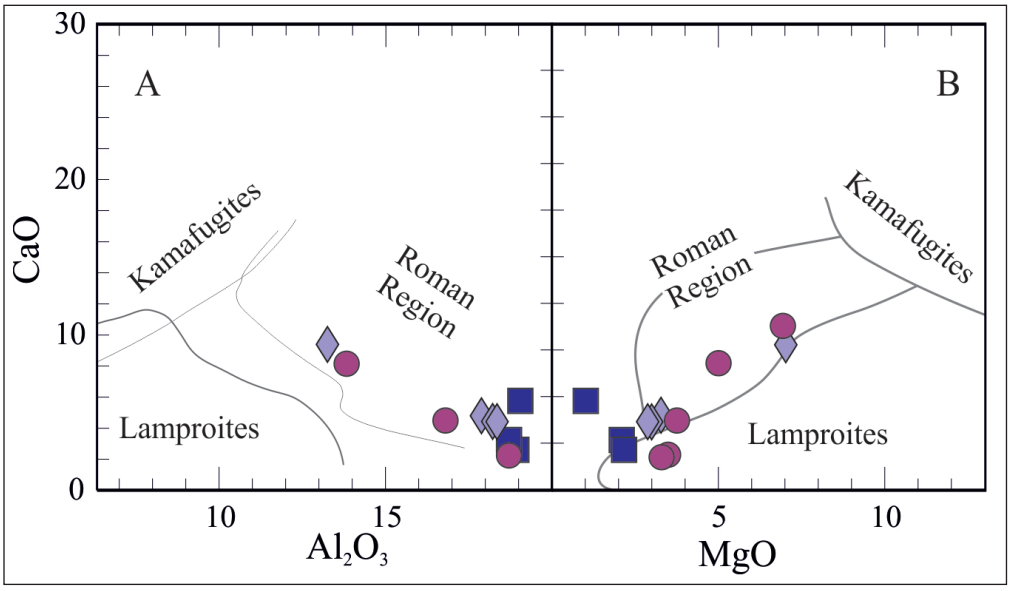

Figure 7- The display of leucitite, minette and trachyte rocks of ALCVS on the classical classification diagram of Foley et al. (1987) for ultrapotassic rocks, a) whole rock CaO % vs. Al_2O_3 % and b) whole rock CaO% vs. MgO% variation diagrams.

ratios (Figure 9 b). High Th/Yb (3.6-8), Ta/Yb (0.2-0.5) and Ba/Th (59.6-156.2) ratios and Th (7.7-17.2 ppm) values observed in all samples (including andesites), suggest a mantle source area which was modified by subduction processes. Another evidence for subduction effect to mantle source comes from negative Ti anomalies on N-MORB normalized multi-element diagrams as it strongly indicates the existence of the Ti-bearing phases such as sphene and rutile in the mantle source region (Figures 8 a-c) (Sun and McDonough, 1989). Besides, the patterns on chondrite normalized multi-element diagrams, suggest that LRE elements significantly enriched compared to HREE, and negative Eu anomaly is negligible (Eu/Eu*=0.83-0.97) (Figures 8 d-f).

7. Differentiation Processes

Trachytes, which are the youngest products of the ALCVS ultrapotassic magmatism within the Pontide forearc basin belt in terms of stratigraphical features and radiochronological data, are also the most evolved members of this magmatism based on their Mg# values (30.22-46.93) and various elemental concentrations (eq. Co: 8.9-9.2 ppm, Ni: 2.9-3.4 ppm). This is best observed on MgO% vs. major and trace element variation diagrams. Trachytes scatter on MgO% vs. SiO_2%, K_2O%, Al_2O_3%, Yb, Th, La and Rb diagrams as the most enriched end members, whereas the most depleted ones on MgO% vs. TiO2, CaO%, Fe_2O_3% and Sc, Co diagrams (Figure 10). This is probably resulted from the fractionation of various minerals. On the other hand, the studies that focus on the related Ne-normative and Qt-normative rocks that were crystallized from single melt, propose that the evolution of magma composition from silica under-saturated to saturated, could only be possible under complicated open system processes (Wilson et al., 1995; Panter et al., 1997).

Tosya region, within the Pontide forearc basin belt, is the area where ultrapotassic trachytes crop out abundantly. Tosya trachytes exhibit the primary contact relationship with metamorphic basement rocks. Trachytic dykes and stocks cut the basement rocks and replace into them differently from Amasya region. In Tosya trachytes accidental quartz originated from basement rocks, are abundant and these samples display quartz-normative composition (Genç et al., 2013).

After evaluating all of the geochemical data of Pontide forearc basin belt ultrapotassic rocks together, it is obvious the ultrapotassic melt differentiation that generate the three lithologies, was achieved by crystallization processes. This is also evident by the MgO% vs. Ta/Zr diagram. The data points of leucititic, lamprophyric and trachytic rocks (taken from Genç et al. 2013) seem to scatter along both of the trend lines resemble FC and AFC processes. The most evolved samples of Amasya trachytes represent the end member products due to the AFC processes whereas leucitites and lamprophyres present no variation on this diagram (Figure 11).

On behalf that the stratigraphical relationships between trachytes with basement rocks and other nepheline-normative ultrapotassic lithologies, with their petrographical features and the geochemical data obtained from Genç et al. (2013), assimilation accompanied during the crystallization of quartz normative trachytes. In order to examine this hypothesis, we modeled adequately AFC processes to answer the question of the degree of crustal assimilation. For this aim, we first decided the best two elements for modeling after checking the correlation coefficients for various elements of our data set and then follow the equations of DePaolo (1981). Therefore the correlation coefficient of these two elements is -0.92, we prefer Co and La. Co, as an compatible element prefer to participate in the solid mineral structure, in contrast La is an incompatible element tend to remain in melt phase. Besides, the sample 11-KT-33 is accepted as to represent the ultrapotassic primitive melt composition. We calculated the possible change of melt composition during the crystallization of hypothetical mineral paragenesis. We also compiled the partition coefficients (K_d) from GERM database. Among the hypothetical fractionation trends on Figure 12, the r_1 curve suggest the lowest crustal assimilation rate. It represents the calculated melt composition based on the $cpx_{0.35} + lc_{0.55} + ph_{0.10}$ mineral paragenesis with $D_{Co} = 3.22$ and $D_{La} = 0.020$ values. The ratio of the crustal assimilant to crystallization rate is up to 1% mostly. The r_2 melt composition is calculated according to the $cpx_{0.25} + am_{0.05} + ph_{0.25} + kf_{0.4} + plg_{0.05}$. mineral composition with $D_{Co} = 6.83$, $D_{La} = 0.022$. The assimilation rate is about 5% in case of r_2 curve of melt composition change. In terms of AFC modeling, it seems that, LCVS ultrapotassic samples tend to follow r_2 curve on La vs. Co diagram (Figure 12) as indicating that the trachytes are the possible products of accompanying assimilation during crystallization in which the rate of assimilant is 5%.

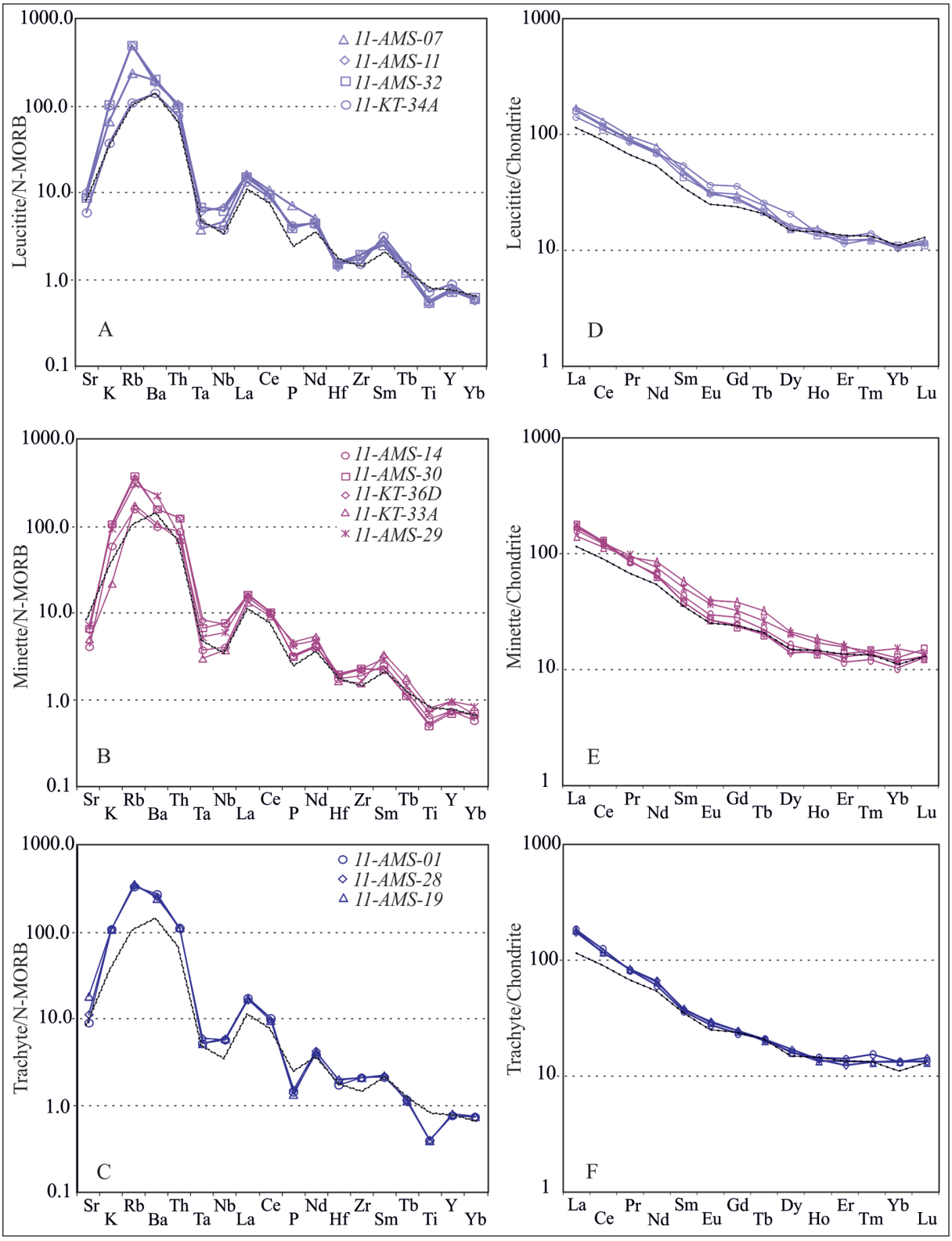

Figure 8- N-MORB and Chondrite normalized multi-element diagrams of ALCVS lava samples (explanations were given within diagrams and text). N-MORB and Chondrite values were taken from Sun and McDonough (1989).

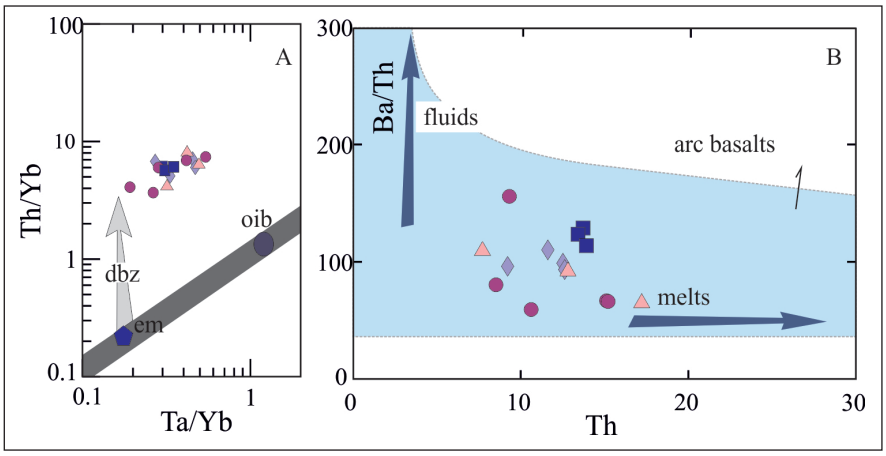

Figure 9- a) The comparison of leucitite, minette and trachyte samples with different source areas in Ta/Yb vs. Th/Yb diagram (Pearce et al., 2005); em and oib areas were taken from Sun and McDonough (1987) (em: enriched source area, oib: oceanic island basalt, dbz: subduction zone enrichment), b) the comparison of samples with arc basalts as the products of subduction modified source areas on Th (ppm) vs. Ba/Th diagram (Hawkesworth et al., 1997).

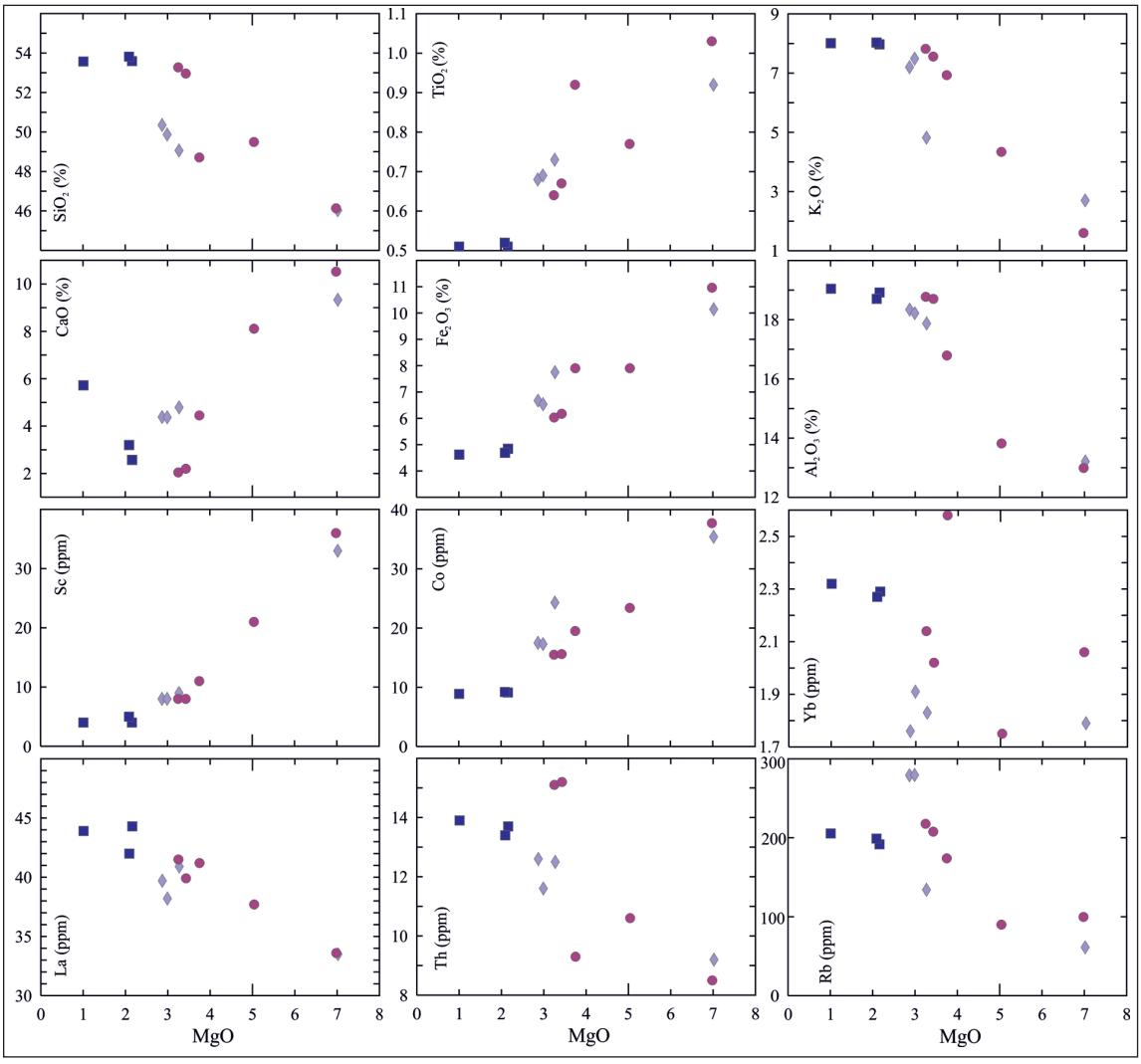

Figure 10- Some major element oxide and trace element variation diagrams MgO (%) values, for the ALCVS lavas.

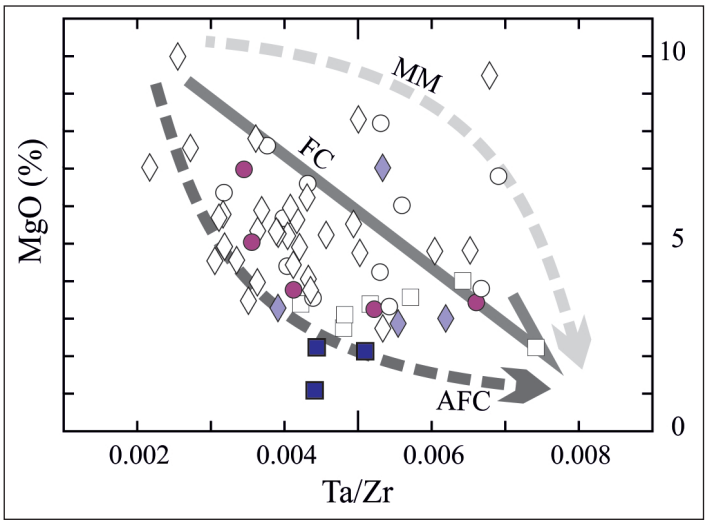

Figure 11- The distribution of samples on Ta/Zr vs. MgO diagram with the expected trend lines fractional crystallization (FC) and assimilation fractional crystallization (AFC) processes. The data for ultrapotassic rocks observed in the belt that continues westward were taken from Genç et al. (2013).

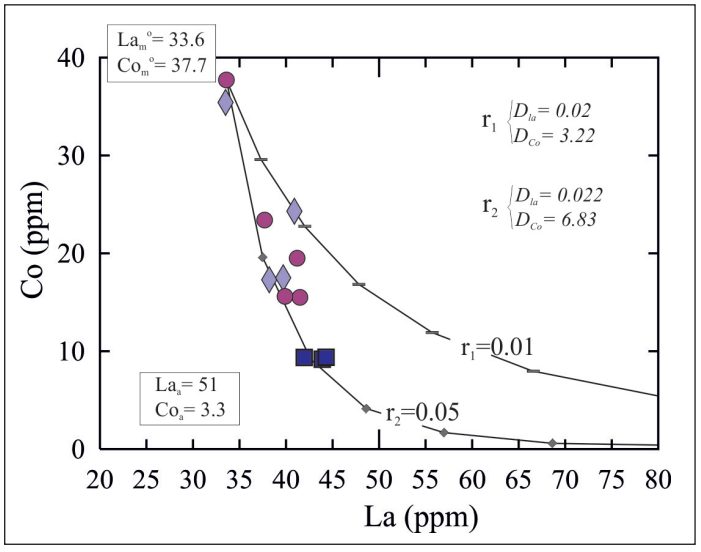

Figure 12- Co vs. La AFC modelling for ALCVS ultrapotassic rocks. See the text for explanations (m: primary melt component, a: pollutant, D: total participation coefficient).

Results

Our main results obtained from this study, are as follows:

- Late Cretaceous ultrapotassic rocks which are observed within Pontide forearc basins, comprise leucitites, minettes and trachytes. Amasya, as a part of Pontide belt, has a significance that it is a location where the all three lithologies coexist.
- Stratigraphical evidences of ALCVS suggest that the ultrapotassic volcanism and deposition of the succession were coeval and the trachytes are the youngest products of this volcanism.
- Radiochronological data is compatible with observations of local stratigraphy as the ultrapotassic volcanism occurred during Campanian time. It also confirms the trachytes are the youngest products of this volcanism.
- The ALCVS ultrapotassic rocks display

geochemical similarities with subduction zone magmatic/volcanic rocks and they associated with each other in time and space due to their common origin, despite they are represented by various lithologies.

- The nepheline normative leucitite and minette type rocks of the ALCVS is evaluated as coeval crystallization products of ultrapotassic melts due to the their field relationships and identical geochemical features (see MgO vs. major and trace element variation diagrams). The differentation between leucitites and minettes, were not controlled by fractional crystallization nor accompanying assimilation processes.
- The differentiation of quartz-normative trachytes which are the youngest products of Late Cretaceous ultrapotassic magmatism, was achieved by assimilation of %5 basement rocks during the crystallization of ultrapotassic melts.

Acknowledgement

This study is a part of the ongoing PhD thesis of Fatma GÜLMEZ (Petrological Evolution and Tectonic Implications of the Late Cretaceous (?) leucite-bearing basalts and lamprophyres of the Ankara-Erzincan Suture Belt). The PhD study was supported by TUBİTAK (Project no: 110Y088) and ITU-BAP Projects coordinated by Prof. Ş. Can GENÇ. The paper refers unpublished data belong to the project with thesis and it cites to abstracts which were presented at international meetings/conferences. We would like to thank to project teams for their contributions in field, office and laboratory studies. We appreciated Prof. Okan TÜYSÜZ as he informed us about the presence of ultrapotassic rocks in Central Pontides.

We would like to thank our TUBİTAK project team members Dr. M. F. Roden (Georgia Univ, USA) and Dr. Z. BİLLOR (Auburn University, USA) for their detailed work on the collection of representative samples for the production of radiochronological data during field studies. We also thank to Assoc. Prof. Yalçın ERSOY for his contributions to AFC modelling.

Received: 04.05.2015
Accepted: 29.05.2015
Published: December 2015

References

Adamia, S. A., Chkhotua, T., Kekelia, M., Lordkipanidze, M., Shavishvili, I., Zakariadze, G. 1981. Tectonics of the Caucasus and adjoining regions: implications for the evolution of the Tethys ocean. *Journal of Structural Geology*, 3(4), pp.437-447.

Alp, D. 1972. Amasya yöresinin jeolojisi. *İ.Ü. Fen Fakültesi Monografileri*, İstanbul, 101 p.

Altherr, R., Topuz, G., Siebel, W., Şen, C., Meyer, H. P., Satır, M., Lahaye, Y. 2008. Geochemical and Sr–Nd–Pb isotopic characteristics of Paleocene plagioleucitites from the Eastern Pontides (NE Turkey). *Lithos* 105(1), pp.149-161.

Asan, K., Kurt, H., Francis, D., Morgan, G. 2014. Petrogenesis of the Late Cretaceous K-rich rocks from the Central Pontide orogenic belt, North Turkey. *Island Arc* 23, pp.102-124.

Baş, H. 1986. Petrology and geochemistry of the Sinop volcanics. *Geological Bulletin of Turkey* 29, 143-56.

Bailey E. B. ve McCallien, W. J. (1950). The Ankara mélange and the Anatolian thrust. *Mineral Research and Exploration Institute of Turkey (MTA) Bulletin* 40, 17-21

Bektaş, O., Gedik, İ. 1988. A new formation with leucite-bearing shoshonitic volcanism in the Kop area (Everekhanları Formation) and its relationship with the evolution of the eastern Pontide arc, NE, Turkey. *Geological Society of Turkey Bulletin* 31, pp.11-19.

Blumenthal, M. M. 1950. Beitreage zur Geologie des Landschaften am Mittleren und untern Yeşilırmak (Tokat, Amasya, Havza, Erbaa, Niksar). *MTA Yayınları*, Seri D, No: 4, Ankara.

Ciobanu, C. L., Cook, N. J., Stein, H. 2002. Regional setting and geochronology of the Late Cretaceous Banatitic magmatic and metallogenetic belt. *Mineralium Deposita*, 37(6-7), pp.541-567.

Conticelli, S., Avanzinelli, R., Poli, G., Braschi, E., Giordano, G. 2013. Shift from lamproite-like to leucititic rocks: Sr–Nd–Pb isotope data from the Monte Cimino volcanic complex vs. the Vico stratovolcano, Central Italy. Chemical Geology. 353, 246-266.

Çapan, U.Z. (1984). Ankara melanjı içindeki zeolitli alkali bazaltik volkanizmanın karakteri ve yaşı hakkında. *Türkiye Jeoloji Kurumu 38. Bilimsel ve Teknik Kurultayı, Bildiri özetleri*: 121–123.

Dalrymple, G.B., Alexander, E.C., Lanphere, M.A., Kraker, G.P. 1981. Irradiation of samples for $^{40}Ar/^{39}Ar$ dating using the geological survey TRIGA reactor. *USGS Professional Paper 1176*, pp.1-55.

DePaolo, D. J. 1981. Trace element and isotopic effects of combined wallrock assimilation and fractional crystallization. *Earth and Planetary Science Letters* 53(2), pp.189-202.

Eyüboğlu, Y. 2010. Late Cretaceous high?K volcanism in the eastern Pontide orogenic belt: Implications for the geodynamic evolution of NE Turkey. *International Geology Review* 52(2-3), pp.142-186.

Foley, S. 1992. Vein-plus-wall-rock melting mechanisms in the lithosphere and the origin of potassic alkaline magmas. Lithos, 28(3), pp.435-453.

Foley, S. F., Venturelli, G., Green, D. H., Toscani, L. 1987. The ultrapotassic rocks: characteristics, classification, and constraints for petrogenetic models. *Earth-Science Reviews 24(2)*, pp.81-134.

Georgiev, S., Marchev, P., Heinrich, C. A., Von Quadt, A., Peytcheva, I., Manetti, P. 2009. Origin of nepheline-normative high-K ankaramites and the evolution of Eastern Srednogorie arc in SE Europe., 50(10), pp.1899-1933.

Gedik., A., Ercan, T., Korkmaz, S. 1983. Orta Karadeniz (Samsun-Sinop) havzası jeolojisi ve volkanik kayaçlarının petrolojisi. *Maden Tetkik ve Arama Genel Müdürlüğü Dergisi* 99, 34-51.

Genç, Ş.C., Tüysüz, O., Karacık, Z., Gülmez, F., Tüysüz, A. 2013. Ankara-Erzincan kenet kuşağı üzerinde yeralan Geç Kretase (?) yaşlı lösitli bazaltlar ile lamprofirlerin petrolojik evrimi ve tektonik anlamı. TÜBİTAK ÇAYDAG Projesi Proje No: 110Y088.

Gülmez, F., Genç, Ş.C., Tüysüz, O., Karacık, Z., Roden, M., F., Billor, M. Z., M. , Hames, W.E. 2014*a*. Geochemistry and petrogenesis of the late Cretaceous potassic-alkaline volcanic rocks from the Amasya Region (northern Turkey), EGU-2013, Vienne, *EGU General Assembly Conference Abstracts* 15, 9833p.

Gülmez, F., Genç, Ş. C., Prelevic, D. 2014*b*. Amasya ve Kalecik civarı Geç Kretase yaşlı alkali volkanik kayalarında taze lösit bulgusu, 67. *Türkiye Jeoloji Kurultayı*, 2014, Ankara, 479p.

Hames, W., Unger, D., Saunders, J., Kamenov, G. 2009. Early Yellowstone hotspot magmatism and gold metallogeny. *Journal of Volcanology and Geothermal Research*, 188(1), pp.214-224.

Hawkesworth, C. J., Turner, S. P., McDermott, F., Peate, D. W., Van Calsteren, P. 1997. U-Th isotopes in arc magmas: Implications for element transfer from the subducted crust. *Science*, 276(5312), pp.551-555.

Koçyiğit, A., Özkan, S., Rojay, B. 1988. Examples from the forearc basin remnants at the active margin of northern Neo-Tethys; development and emplacement ages of the Anatolian Nappe, Turkey. *Middle East Technical University, Ankara-Turkey* 21(1), pp.183-220.

Le Bas, M. J., Le Maitre, R. W., Streckeisen, A., Zanettin, B. 1986. A chemical classification of volcanic rocks based on the total alkali-silica diagram. *Journal of Petrology* 27(3), pp.745-750.

Le Maitre, R. W. 2002. Igneous Rocks: A Classification and Glossary of Terms: A Classification and Glossary of Terms: Recommendations of the International Union of Geological Sciences, Subcommission on the Systematics of Igneous Rocks. *Cambridge University Press UK*, 193 p.

Ludwig, K.R. 2003. User's manual for Isoplot, v. 3.0, a geochronological tool kit for Microsoft Excel. *Berkeley Geochronological Center,* Berkeley, 75 p.

Luhr, J.F., Kyser, T.K. 1989. Primary igneous analcime; Colima minettes. *American Mineralogist* 74 (1-2), pp.216-223.

McKenzie, D. 1989. Some remarks on the movement of small melt fractions in the mantle. *Earth and Planetary Science Letters* 95(1), pp.53-72.

Mederer, J., Moritz, R., Ulianov, A., Chiaradia, M. 2013. Middle Jurassic to Cenozoic evolution of arc magmatism during Neotethys subduction and arc-continent collision in the Kapan Zone, southern Armenia. *Lithos*, 177, pp. 61-78.

Mitchell, R.H., Bergman, S.C. 1991. Petrology of lamproites. *Springer NY*, 446 p.

Nelson, D.R. 1992. Isotopic characteristics of potassic rocks: evidence for the involvement of subducted sediments in magma genesis. *Lithos* 28(3), pp.403-420

Okay, A. I., Şahintürk, O. 1997. Regional and Petroleum Geology of the Black Sea and Surrounding Region. *AAPG Memoir* 68, pp.291-312.

Okay, A.I., Tüysüz, O. 1999. Tethyan sutures of northern Turkey. *Geological Society London*, Special Publications 156(1), pp.475-515.

Panter, K. S., Kyle, P. R., Smellie, J. L. 1997. Petrogenesis of a phonolite–trachyte succession at Mount Sidley, Marie Byrd Land, Antarctica., 38(9), pp.1225-1253.

Pearce, J. A., Stern, R. J., Bloomer, S. H., Fryer, P. 2005. Geochemical mapping of the Mariana arc?basin system: Implications for the nature and distribution of subduction components. *Geochemistry, Geophysics, Geosystems* 6(7), Q07006, doi:10.1029/2004GC000895

Reading, H. G. (Ed.) 2009. Sedimentary environments: processes, facies and stratigraphy. *John Wiley and Sons*, 704 p.

Rock, N. M. 1991. Lamprophyres. Blackie, *Glasgow, UK*. 285 p.

Rojay, B. 1995. Post-Triassic evolution of Central Pontides: evidence from Amasya region, northern Anatolia., 31, pp.329-350.

Sosson, M., Rolland, Y., Müller, C., Danelian, T., Melkonyan, R., Kekelia, S., Adami, S., Babazadeh, V., Kangarli, T., Avagyan, A., Galoyan, G., Mosar, J. 2010. Subductions, obduction and collision in the Lesser Caucasus (Armenia, Azerbaijan, Georgia), new insights. *Geological Society London, Special Publications*,340(1), pp.329-352.

Sun, S., McDonough, W.F. 1989. Chemical and isotopic systematics of oceanic basalts: implications for mantle composition and processes. Saunders, A.D., Norry, M.J. (Eds.),Magmatism in the ocean basins. *Geological Society Special Publication* 42, pp. 313-345

Şengör, A. M.C., Yılmaz, Y. 1981. Tethyan evolution of Turkey: a plate tectonic approach. *Tectonophysics* 75(3), pp.181-241.

Şengör, A. M. C., Tüysüz, O., İmren, C., Sakınç, M., Eyidoğan, H., Görür, N., Le Pichon, X., Rangin, C. 2005. The North Anatolian fault: A new look. *Annu. Rev. Earth Planet. Sci*.,33, pp.37-112.

Tankut, A., Dilek, Y. ve Önen, P. (1998). Petrology and geochemistry of the Neo-Tethyan volcanism as revealed in the Ankara melange, Turkey. *Journal of Volcanology and Geothermal Research*, 85(1), 265-284.

Topuz, G., Göçmengil, G., Rolland, Y., Çelik, Ö. F., Zack, T., Schmitt, A. K. 2013. Jurassic accretionary complex and ophiolite from northeast Turkey: No evidence for the Cimmerian continental ribbon. *Geology* 41(2), pp.255-258.

Tüysüz, O. 1996. Geology of Amasya and surroundings. *11th Petroleum Congress of Turkey*, Proceedings, Ankara, pp.32-48.

Tüysüz, O., Dellaloğlu, A. A. ve Terzioğlu, N. (1995). A magmatic belt within the Neo-Tethyan suture zone and its role in the tectonic evolution of northern Turkey. *Tectonophysics*, 243(1), 173-191.

Varol, E. (2013). The derivation of potassic and ultrapotassic alkaline volcanic rocks from an orogenic lithospheric mantle source: the case of the Kalecik district, Ankara, Central Anatolia, Turkey. *Neues Jahrbuch für Mineralogie-Abhandlungen*, 191(1), 55-73.

Wilson, M., Downes, H., Cebriar, J. M. 1995. Contrasting fractionation trends in coexisting continental alkaline magma series; Cantal, Massif Central, France. *Journal of Petrology* 36(6), pp.1729-1753.

Yagi, K., Ishikawa, H., Kojima, M. 1975. Petrology of a lamprophyre sheet in Tanegashima Islands, Kagoshima Prefecture, Japan. *Journal of. Japan Association of Mining, Petroleum and Economic Geologist* 70 (7), pp.213-224.

Yılmaz, Y., Tüysüz, O., Yiğitbaş, E., Genç, Ş.C. Şengör, A.M.C. 1997. Geology and tectonic evolution of the Pontides, In: A.G. Robinson (Ed.) Regional and Petroleum Geology of the Black Sea and Surrounding Region. AAPG Memoir 68, pp.183-226.